Effect of physical aging on fracture behavior of Te 2 As 3 Se 5 glass fibers

Guang Yang, Hongfei Chen, Catherine Boussard-Plédel, Jean-Christophe Sangleboeuf, Bruno Bureau

Effect of physical aging on fracture behavior of $Te_2As_3Se_5$ glass fibers

Guang Yang[1, 2, 3*], Hongfei Chen[1], Catherine Boussard-Plédel[2], Jean-Christophe Sangleboeuf[3*], Bruno Bureau[2]

[1] School of Materials Science and Engineering, Shanghai University, Shangda Rd. 99, Baoshan, Shanghai 200444, China

[2] Verres et Céramiques, UMR CNRS 6226 Sciences Chimiques de Rennes, Université de Rennes 1, 35042 Rennes cedex, France

[3] Département Mécanique&Verres, Institut de Physique de Rennes, UMR CNRS 6251, Université de Rennes 1, 35042 Rennes cedex, France

Abstract

Fracture surface characteristics of $Te_2As_3Se_5$ (TAS) glass fibers aged in light and in dark have been investigated respectively for understanding physical aging effect on their fracture behavior. The properties including tensile strength (σ), surface flaw depth (α), and mirror radii (r_m) were measured by DY30 Adamel Lomarghy and SEM respectively. Shape factor extracted by fitting of σ vs α confirms that fractures of fibers aged in dark for 4 months originate from their surface flaw, but it does not work for fibers aged in light for 4 months. However, mirror constants ($=\sigma r_m^{1/2}$) of fracture surface for the TAS glass fibers aged in dark are in a good agreement with those aged in light. One possible reason is that the photoinduced effect changes the structure of glass surface during the physical aging.

Keywords: Fracture, shape factor, glass fiber, chalcogenide glass

1. Introduction

* Corresponding author: guangyang@shu.edu.cn; jean-christophe.sangleboeuf@univ-rennes1.fr;

Chalcogenide glasses possess large transparency in the infrared (IR) range, covering two atmosphere windows (2-12 μm), as well as their good thermo-mechanical properties which make the glass easy to be drawn into fibers [1-3]. The glass with TAS composition shows a large domain of transmission in the mid-IR from 800-4000 cm^{-1} with a minimum for the attenuation of 1dB/m and an excellent resistance to devitrification during fiber drawing process [4-7]. Therefore TAS fibers have been used as bio-sensor for medical and environmental detections [4, 8, 9]. Structure of TAS glasses are based on a two dimensional glass network where atomic As is bridged by chalcogen chain fragments, and introduction of tellurium in TAS glasses induces breaking of chalcogen chain and formation of $AsSe_{3-x}Te_x$ pyramidal units[10-12]. Our previous researches have reported that the surface quality of TAS fibers, physical aging conditions, such as light, load and air, and glass structural relaxation, have effect on the σ [5, 7, 13]. However, so far for TAS glass fibers there is little report about correlation between the σ and α or r_m under different aging conditions. In this work, we carried out a detail research on the correlation between the σ and α or r_m for TAS fibers aged in light and in dark respectively.

2. Experiments

TAS fibers were drawn from glass pre-forms synthesized in vacuum from high purity raw materials. Elementary substances, selenium and arsenic, were further purified to eliminate the remaining oxygen and hydrogen with the volatilization technique by heating at 240 and 290 ^oC respectively under vacuum for several hours. The required amounts of Te, As and Se were sealed in a special silica tube under vacuum and sublimated (at 800 ^oC), to remove carbon and compounds with higher boiling points. The mixture was maintained at 750 ^oC for 12 h in a rocking furnace to ensure a good homogenization of the liquid. Then the ampoule was quenched in water

and annealed at 120 ^{o}C, near the glass transition temperature for 2 hours. The obtained samples had a 1.0 cm large diameter and were 10.0 cm long. The glassy nature of the obtained glassy preform rod was confirmed by X-ray dispersion analysis (Philips PW3230, Philips, Almedo, Netherlands). The infrared optical homogeneity of the preform rod and the quality, including the absence of some obvious crystals and bubbles, were verified with a thermal-imaging camera (FLIR PM 390 ThermaCAM, FLIR Inframetrics, Portland, OR).

Optical fiber was drawn from a home-made drawing tower with a protection gas flow (He, 2.5 L/min) as shown in Figure 1. The fiber velocity, diameter, tension, and helium flow velocity, as well as the average furnace temperature, were continuously monitored (data recording frequency of 1 Hz) [14]. The fiber diameter was measured using a laser interferometer. Glass cylinders are heated up to the softening temperature at 290 ^{o}C, and flowed to the appropriate diameter by tuning both the temperature (and thus the viscosity) and the drawing speed. The diameters of the fiber had been made about 400 μm. The fiber was fixed into a special drum, which was separated into many parts with some rungs and each part of which was with a length of 13 cm to keep fiber without any touch with the drum. After the fiber was synthesized, they were immediately stored individually in three conditions: in dark, and in light (fluorescent tubes on one side of fibers), for 0.5, 1.5, 3, 4 and 5 months respectively at room temperature and under atmosphere. Thus, some surface abrasion could induce fracture-initiating flaws during fiber drawing process, but no more surface abrasion occurs after fiber drawing and during fiber storage. They were tested in tension after physical aging for different periods of time at room temperature and in air.

Tensile tests were carried out on a DY30 Adamel Lomarghy testing machine (DY 30 Adamel Lhomargy, MTS Systems, Ivy sur Seine, France). Fibers were end-tabbed to prevent against sliding and/or indentation. Alignment was optimized on a set of fibers prior to testing. Displacement controlled experiments were conducted on specimens with 7.0 cm long gauges, using a 100 N load cell (precision of 0.1 N), a cross head speed of 1.0 mm/min (apparent deformation rate 2.4×10^{-4} s^{-1}). After tensile tests, the TAS fiber's surface and fracture surface were characterized using SEM (JSM6301F, JEOL, Tokyo, Japan). From these SEM images, all parameters in Figure 2 (α and r_m) of fracture surface were measured by a Quartz PCI Lite/Satellite Image Acquisition software (Quartz PCI, Quartz Imaging Corporation, Vancouver, Canada).

3. Results and discussion

3.1. Initial defects

Figure 2 shows the typical fracture surface with general appearance of fracture mirror and other related features on silicate fibers. It has been demonstrated that the failure begins from an initial and small surface flaw with depth α on surface of silicate fibers, then the crack promptly propagates through the fiber, giving birth to three distinct regions of fracture features named as the mirror, mist and hackle [15-17].

For a sharp flaw on fiber's surface, where the flaw size is considered small compared with the radius of the glass fiber, the strength σ and flaw depth α can be related as [15]:

$$K_{IC} = Y\sigma\sqrt{\pi\alpha} \quad (1)$$

where Y is shape factor depending on initial crack geometry (the initial flaw depth α) and its size in relation to the fiber radius r, and K_{IC} is toughness of bulk glass. There are two simplified cases of Y, including a semi-circular flaw in an infinite body with a constant value of Y=0.64 and a

straight surface cracks in an infinite body with Y=1.126 [15-17]. Figure 3 shows the tensile strength vs the initial flaw depth. First of all, due to the similar failure behavior, we fitted both conditions, viz. in dark and in light, in one way which can be expressed as:

$$\sigma = 1.8\times10^{5} / \ (1.07\sqrt{\pi\alpha}) \qquad (2)$$

But we observed an invalid adjusted coefficient of determination, $R^2 \approx$ -0.23. The mathematically invalid fitting could be caused by mixture of points with different aging conditions. Thus, we have fitted the tensile stress vs the initial flaw depth of TAS fibers for samples aged in light and in dark respectively, as shown in Figure 3. With our experimental K_{IC} (0.18 ± 0.05MPa.m$^{1/2}$) of bulk TAS glass, the Y are obtained as 0.83 in dark condition and 1.34 in light condition respectively. The Y equaling to 0.83 for dark condition lies well within the region of (0.668, 1.126), which means the fracture originates from initial flaw on sample's surface. But the Y (1.34) for fibers aged in light is obviously beyond the region. However, from the SEM images of fibers aged in light, those aged in dark and even those of fresh fibers, most their fracture surfaces are similar as in Figure 2. On one side, this excludes an important effect from glass structure relaxation with physical aging in light or in dark conditions for all fibers. On the other side, this could be correlated to photoinduced effect on the surface of TAS fibers with a depth about several microns, which is covering the initial flaws [18-21]. It could be explained as that the photoinduced effect changes local glass structure (within fiber's surface) during the physical aging, as mentioned by many previous researches on chalcogenide glasses [18-21]. The variation of the local structure could induce decaying of K_{IC} in light condition. For example, if we suppose that fracture behavior of fibers aged in light and in dark have a same Y (0.83), then the K_{IC} could decay from 0.18 ± 0.05MPa.m$^{1/2}$ to 0.13 ± 0.05MPa.m$^{1/2}$. And the adjust R^2 are 0.78 and 0.70, which are mathematically valid and

much better than -0.23 of the blue solid fitting in Figure 3. Furthermore details about variation about the σ during physical aging in the two conditions can be found in our previous paper [13].

Additionally, new defects (the maximum size is about 100 nm in Figure 4), which may result from a reaction between fiber and water or O_2 during physical aging, is much smaller than the dimension, 2b, of initial flaw within the range from 2 to 10 μm as shown in Figure 5(b). This confirms that the fracture does not originate from the new defects appearing after physically aged in two conditions.

3.2. Mirror region

Most fracture surfaces have similar mirror regions with semi-circular shapes. It has been extensively demonstrated the product of fiber strength σ and the square root of the mirror radius r_M (inner mirror radius) or the mist radius r_H (outer mirror radius) is constant in silicate glasses [15, 22, 23]:

$$\sigma(r_M)^{1/2} = A_1 \quad (3)$$

$$\sigma(r_H)^{1/2} = A_2 \quad (4)$$

where A_1 and A_2 are the so-called mirror constants. From the above equations, the size of the mirror region relates to strength of fiber, viz., higher strength fiber has smaller fracture mirror region.

Figure 6 shows the plots of tensile stress vs inner and outer mirror size for fibers aged 4 months in light and in dark respectively. The mirror constants of TAS fibers (inner 0.33 ± 0.01MPa $m^{1/2}$ and outer 0.39 ± 0.01 MPa $m^{1/2}$ for dark condition, and inner 0.33 ± 0.01MPa $m^{1/2}$ and outer 0.40 ± 0.01 MPa $m^{1/2}$ for light condition) are close to those of As_2S_3 fibers (inner 0.56 MPa $m^{1/2}$, and outer 0.65 MPa $m^{1/2}$) or those of $Ge_{33}As_{12}Se_{55}$ fibers (inner 0.55 MPa $m^{1/2}$, and

outer 0.65 MPa $m^{1/2}$) with low strength, but less than those of SiO_2 fibers (inner 2.23 MPa $m^{1/2}$, and outter 2.42 MPa $m^{1/2}$) with enhanced strength [22]. The minima mirror constants of TAS fibers are due to the weakest bond energy among above four compositions. The bond energy of Te-Se, As-Se, As-S, Ge-Se, and Si-O are 170, 177, 198, 215, and 369 kJ/mol respectively, which are well in consistent with above result [24]. Both of mirror constants determined from experiments show good R^2 ($\approx$ 0.91 and 0.81 of inner mirror constants, while 0.92 and 0.83 of outer mirror for fibers aged in dark and in light conditions respectively). Figure 6 exhibits that the fitting results of fibers aged in dark condition for inner and outer mirror constant are in a good agreement with those of fiber aged in light. Even we could do fitting of the two conditions in one curve, because the photoinudced effect only influences on a few micron of fiber's surface [18-20]. Here we just exhibits the data of fibers aged for 4 months, because we do not have enough data for other aged times and they will be researched in future.

The present work shows that the fracture surface pattern of TAS fibers (aged in dark or light) can be divided into three types of failure pattern. First type of failure of the fracture surface is major feature as shown in Figure 5(a) ((b) is enlargement of the mirror region), which is similar to that of silicate glassy fibers in Figure 2. Figure 5(b) also exhibits that the initial flaw could be a particle or a tiny crack on the surface of fiber samples, which may be due to defects on preform-rod formed when polishing with alumina powder or contacting with pulley during drawing process [5]. Usually the sample with first type failure indicates higher stress with smaller size of mirror and even with a wave-like pattern (Figure 5(a)), while lower stress with larger size of mirror and without a wave-like pattern. Compared with fracture surface of fibers aged in dark, however, no evidence could be obtained from SEM images for photoinduced effect on initial flaw

of fibers aged in light. The second type of failure (Figure 5(c)) reveals smooth fiber breakage without any indication of a surface fault. Unfortunately, it is not possible to confirm that we are indeed looking at the original fracture surface for these fibers with smooth fracture patterns because these fibers break into more than 2 parts during test. Therefore the fracture surfaces could well be a result of secondary breaks caused by bending of the fiber during fracture. The last type of failure (Figure 5(d)) is the least appearance of the failure type with a whole circular inside fiber, but fracture seems to originate from insider in fiber instead of an initial surface flaw.

4. Conclusions

The experimental shape factor confirms that the fracture of fibers aged in dark originates from the initial flaw on fiber's surface for fibers aged in light rather than the new defects generated during physical aging, but it is not same in light condition due to the photoinduced effect on the change of fiber's surface structure. However, mirror constants of fibers aged in two conditions determined from experiments are similar, because the photoinudced effect only influences on a few micron of fiber's surface. The fracture surfaces of fibers are divided into three types of failure pattern: with mirror region on the edge of fiber's fracture surface, with mirror region inside of fiber's fracture surface, and no mirror region. Further research on K_{IC} and the mirror constants will be carried out by longer time (1 year or more) physical aging.

Acknowledgments

The authors wish to express their gratitude to Thierry Jouan, and Thierry Pain (Verres et Céramiques, UMR 6226, Université de Rennes 1).

References

[1] A. Zakery, and S. R. Elliott, Optical properties and applications of chalcogenide glasses: a review, Journal of Non-Crystalline Solids 330 (2003) 1-12.

[2] B. J. Eggleton, B. Luther-Davies, and K. Richardson, Chalcogenide photonics, Nature Photonics 5 (2011) 141-148.

[3] W. Gao, M. El Amraoui, M. Liao, H. Kawashima, Z. Duan, D. Deng, T. Cheng, T. Suzuki, Y. Messaddeq, and Y. Ohishi, Mid-infrared supercontinuum generation in a suspended-core As2S3 chalcogenide microstructured optical fiber, OPTICS EXPRESS 21 (2013) 9573-9583.

[4] J. Keirsse, C. Boussard-Plédel, O. Loreal, O. Sire, B. Bureau, B. Turlin, P. Leroyer, and J. Lucas, Chalcogenide glass fibers used as biosensors, Journal of Non-Crystalline Solids 326-327 (2003) 430-433.

[5] C. Pouvreau, M. Drissi-Habti, K. Michel, B. Bureau, J. C. Sangleboeuf, C. Boussard-Pledel, T. Rouxel, and J. L. Adam, Mechanical properties of a TAS fiber: a preliminary study, Journal of Non-Crystalline Solids 316 (2003) 131-137.

[6] V. S. Shiryaev, M. F. Churbanov, E. M. Dianov, V. G. Plotnichenko, J. Adam, and J. Lucas, Recent progress in preparation of chalcogenide As-Se-Te glasses with low impurity content, Journal of Optoelectronics and Advanced Materials 7 (2005) 1773-1779.

[7] G. Delaizir, J. C. Sangleboeuf, E. A. King, Y. Gueguen, X. H. Zhang, C. Boussard-Pledel, B. Bureau, and P. Lucas, Influence of ageing conditions on the mechanical properties of Te-As-Se fibres Journal of Physics D: Applied Physics 42 (2009) 0954051-0954056.

[8] P. Lucas, M. R. Riley, C. Boussard-Plédel, and B. Bureau, Advances in chalcogenide fiber evanescent wave biochemical sensing, Analytical Biochemistry 351 (2006) 1-10.

[9] M.-L. Anne, J. Keirsse, V. Nazabal, K. Hyodo, S. Inoue, C. Boussard-Pledel, H. Lhermite, J. Charrier, K. Yanakata, O. Loreal, J. Le Person, F. Colas, C. Compère, and B. Bureau, Chalcogenide Glass Optical Waveguides for Infrared Biosensing, Sensors 9 (2009) 7398-7411.

[10] H.-L. Ma, X.-H. Zhang, J. Lucas, H. Senapati, R. Bohmer, and C. A. Angell, Covalent bond connectivity, medium range order, and physical properties in TeX and TeXAs glasses, Journal of Solid State Chemistry 96 (1992) 181-191.

[11] G. Delaizir, M. Dussauze, V. Nazabal, P. Lecante, M. Doll, P. Rozier, E. I. Kamitsos, P. Jovari, and B. Bureau, Structural characterizations of As-Se-Te glasses, Journal of Alloys and Compounds 509 (2010) 831-836.

[12] R. I. Alekberov, S. I. Mekhtiyeva, G. A. Isayeva, and A. I. Isayev, Raman scattering in As-Se-S and As-Se-Te Chalcogenide vitreous semiconductors, Semiconductors 48 (2014) 800-803.

[13] G. Yang, J.-C. Sangleboeuf, C. Boussard-Plédel, and B. Bureau, Effect of Physical Aging Conditions on the Mechanical Properties of Te2As3Se5 (TAS) Glass Fibers, Journal of the American Ceramic Society 96 (2013) 464-468.

[14] G. Yang, T. Rouxel, J. Troles, B. Bureau, C. Boussard-Plédel, P. Houizot, and J.-C. Sangleboeuf, Viscosity of As_2Se_3 Glass During the Fiber Drawing Process, Journal of the American Ceramic Society 94 (2011) 2408-2411.

[15] S. Feih, A. Thraner, and H. Lilholt, Tensile strength and fracture surface characterisation of sized and unsized glass fibers, Journal of Materials Science 40 (2005) 1615-1623.

[16] W. T. Koiter, Rectangular Tensile Sheet With Symmetric Edge Cracks, Journal of Applied Mechanics 32 (1965) 237-237.

[17] D. A. Krohn, and D. P. H. Hasselman, Relation of Flaw Size to Mirror in the Fracture of Glass, Journal of the American Ceramic Society 54 (1971) 411-411.

[18] A. E. Owen, A. P. Firth, and P. J. S. Ewen, Photo-induced structural and physico-chemical changes in amorphous chalcogenide semiconductors, Philosophical Magazine B 52 (1985) 347-362.

[19] K. Shimakawa, A. Kolobov, and S. R. Elliott, Photoinduced effects and metastability in amorphous semiconductors and insulators, Advances in Physics 44 (1995) 475-588.

[20] G. Yang, H. Jain, A. Ganjoo, D. Zhao, Y. Xu, H. Zeng, and G. Chen, A photo-stable chalcogenide glass, Optics Express 16 (2008) 10565-10571.

[21] Y. Gueguen, J. C. Sangleboeuf, V. Keryvin, E. Lepine, Z. Yang, T. Rouxel, C. Point, B. Bureau, X.-H. Zhang, and P. Lucas, Photoinduced fluidity in chalcogenide glasses at low and high intensities: A model accounting for photon efficiency, Physical Review B 82 (2010) 134114.

[22] J. J. Mecholsky, R. W. Rice, and S. W. Freiman, Prediction of Fracture Energy and Flaw Size in Glasses from Measurements of Mirror Size, Journal of the American Ceramic Society 57 (1974) 440-443.

[23] E. B. Shand, Breaking Stress of Glass Determined from Dimensions of Fracture Mirrors, Journal of the American Ceramic Society 42 (1959) 474-477.

[24] L. Pauling, *The Nature of the Chemical Bond,* Cornell University Press, Third ed., Ithaca, NY, 1960.

Figure Captions:

Fig. 1. A custom built fiber drawing set-up.

Fig. 2. A typical enlargement of the initial fracture part.

Fig. 3. Tensile strength vs initial flaw depth of TAS fibers aged in dark and in light for 4 months respectively. Their fitting are blue solid curve for dark and light mixing condition, black dash curve for dark condition, and red dot curve for light condition respectively.

Fig. 4. Surfaces of TAS fibers fresh (left), aged for 1.5 months in light (middle), and aged for 3 months in light (right).

Fig. 5. Fracture surfaces of TAS fibers after physical aging. (a) is the first type failure aged for 1.5 months in light, and (b) is enlargement of the initial fracture part of (a). (c) is the second type failures aged for 5 months in light. (d) is the third type aged for 0.5 months in light.

Fig. 6. Tensile stress vs inner mirror radius (a) and outer mirror radius (b) of TAS fibers in dark (black solid square) and in light (red solid circle) aged for 4 months. Their fitting are black solid curves for dark condition and red dash curves for light condition.

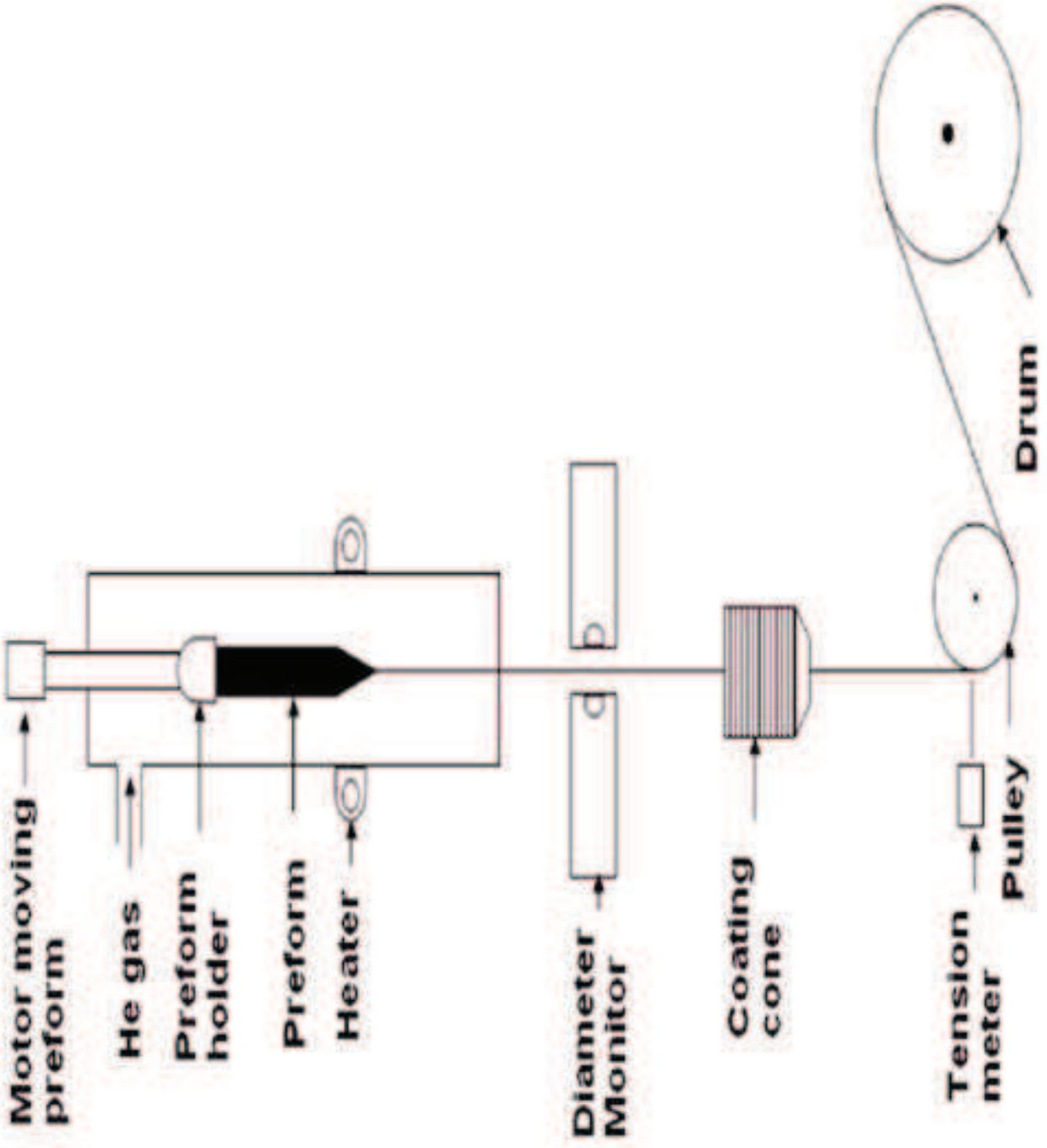
Motor moving preform
He gas
Preform holder
Preform
Heater
Diameter Monitor
Coating cone
Tension meter
Pulley
Drum

Figure

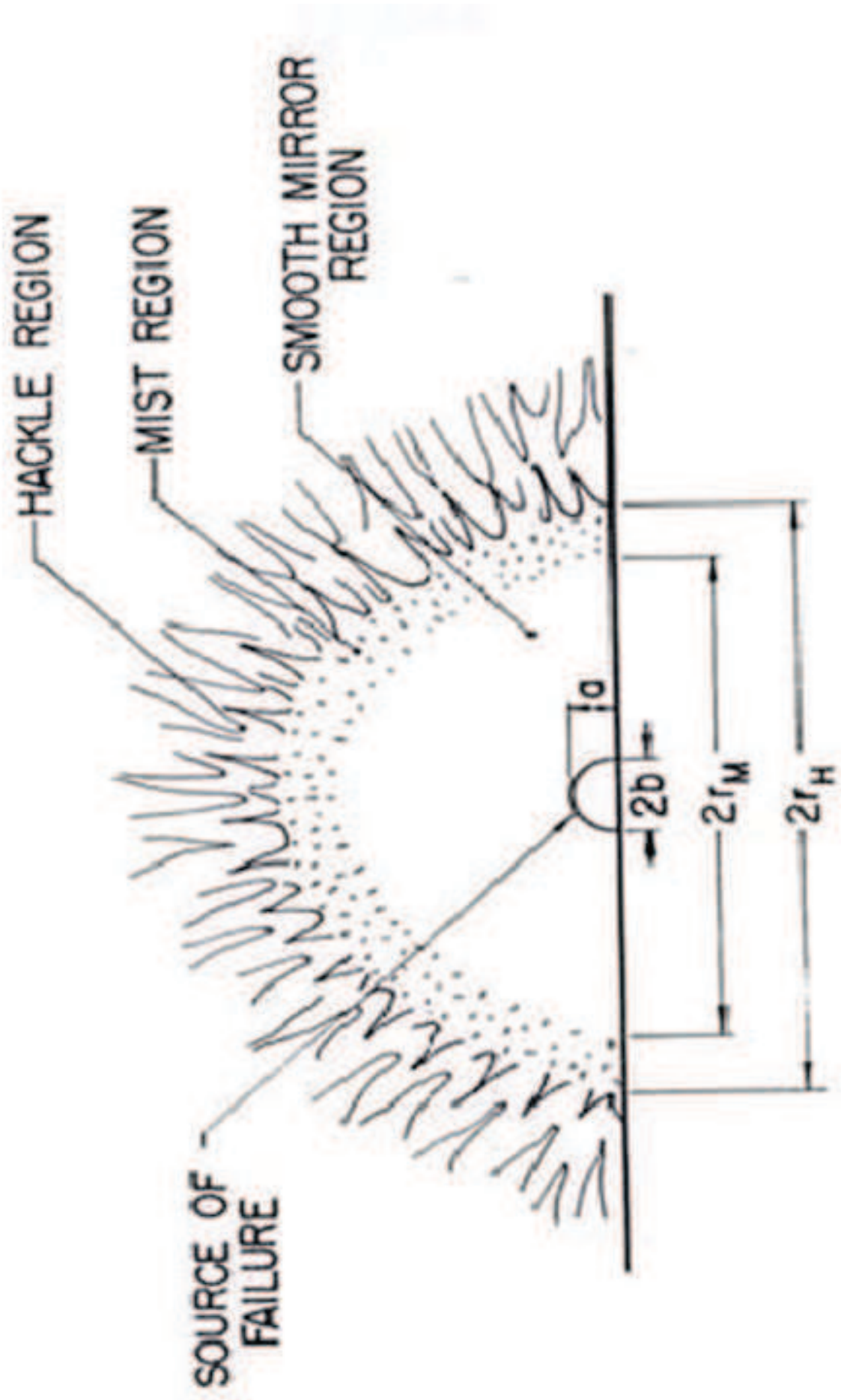

Figure

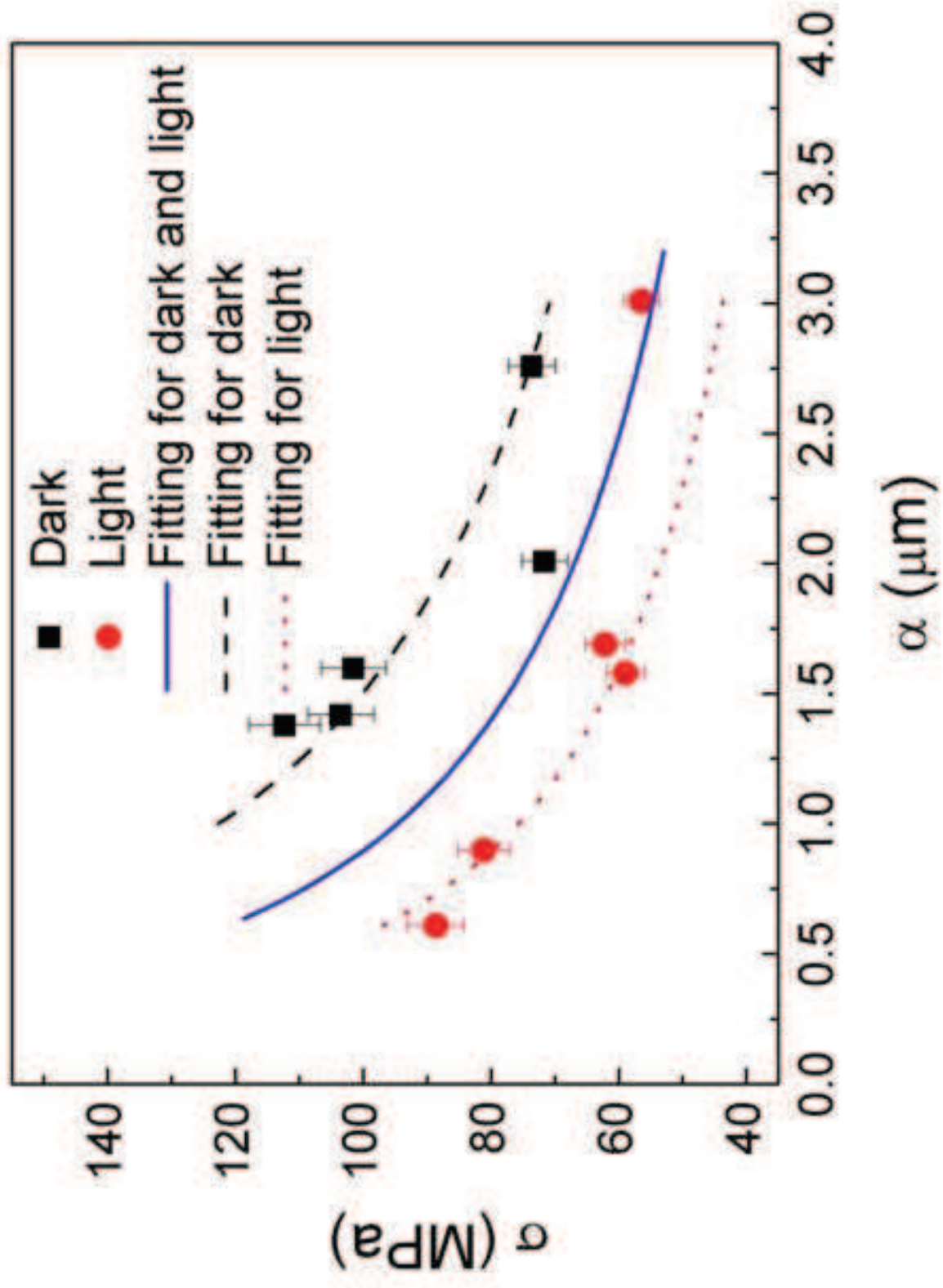
Dark
Light
Fitting for dark and light
Fitting for dark
Fitting for light
σ (MPa)
α (μm)
140
120
100
80
60
40
0.0
0.5
1.0
1.5
2.0
2.5
3.0
3.5
4.0

Figure

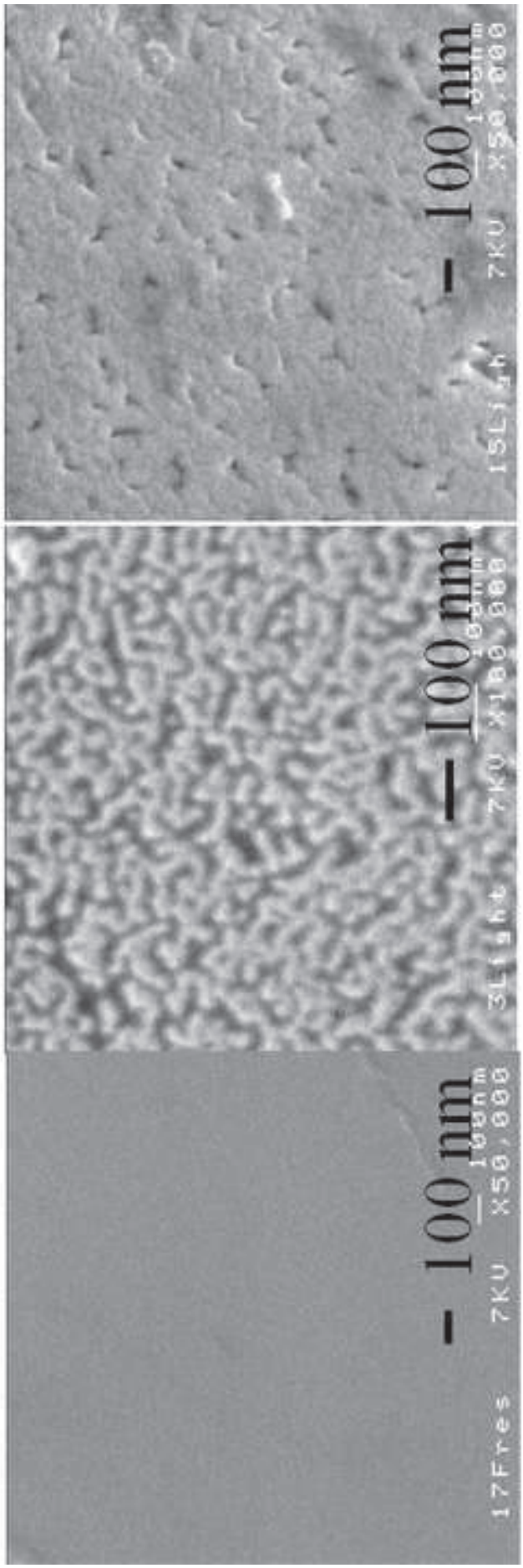
100 nm
17Feb15 7KU X50,000 100nm
100 nm
3L1144 7KU X100,000 100nm
100 nm
15L144 7KU X50,000 100nm

Figure

Figure

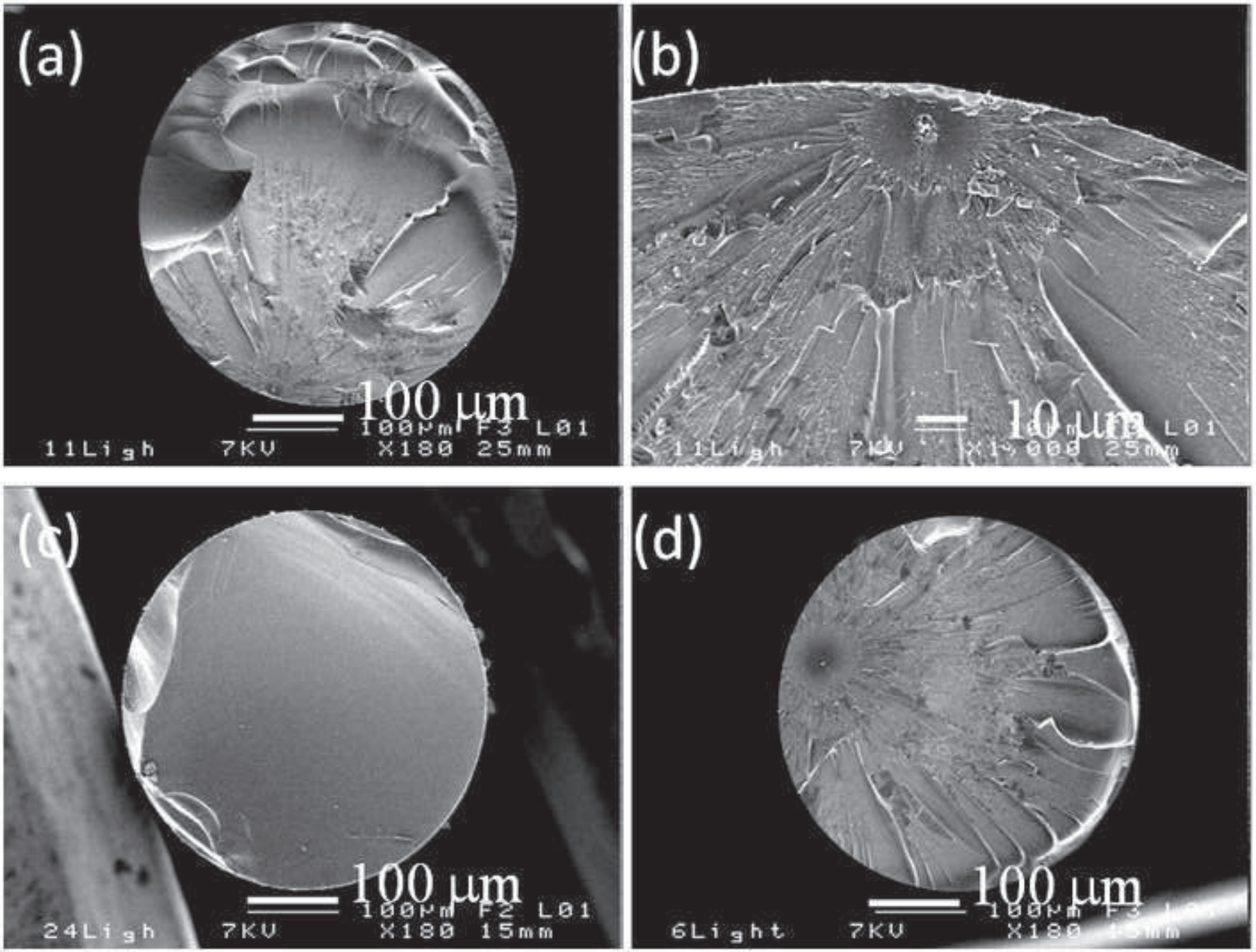

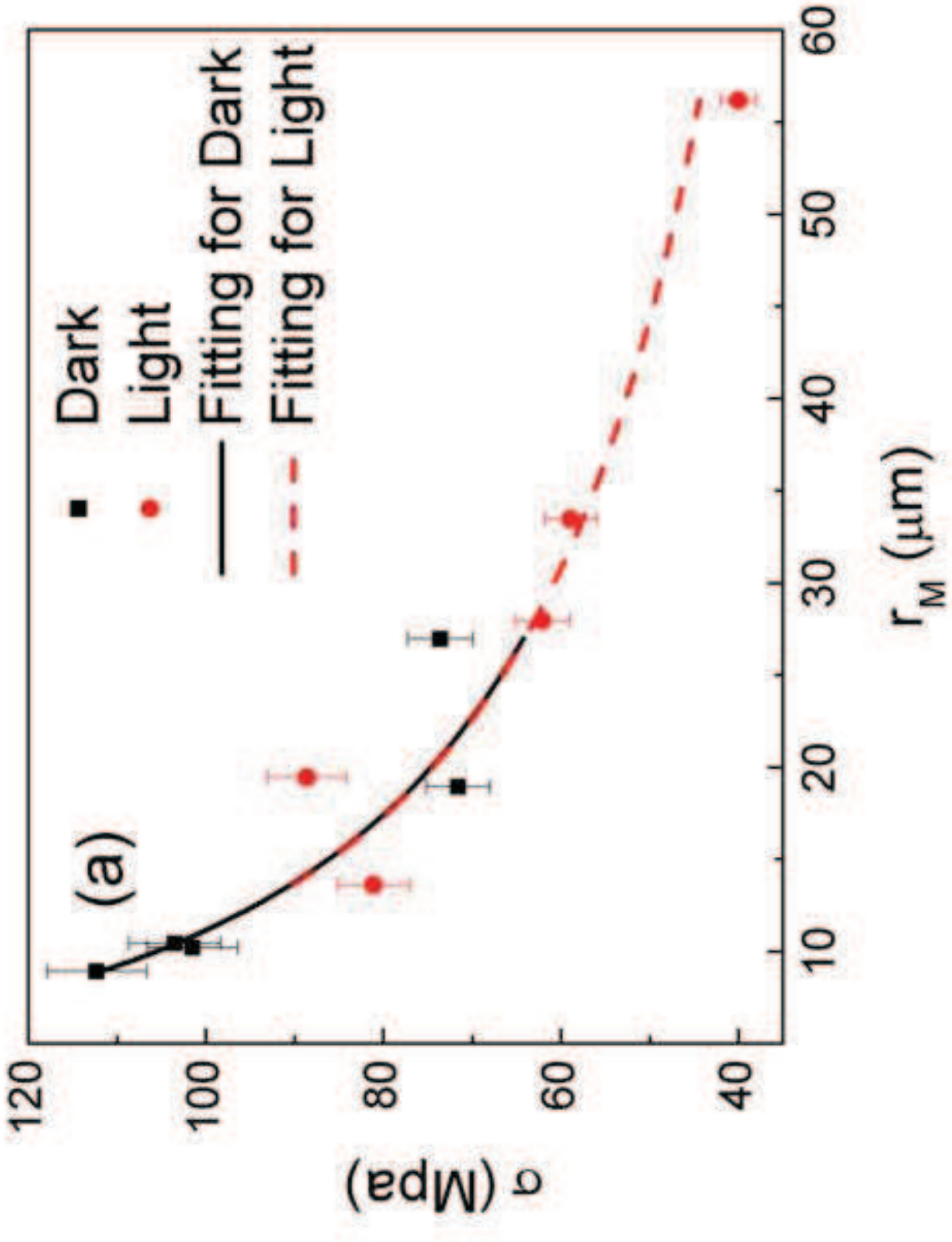
(a)
Dark
Light
Fitting for Dark
Fitting for Light
σ (Mpa)
120
100
80
60
40
10
20
30
40
50
60
r_M (μm)

Figure

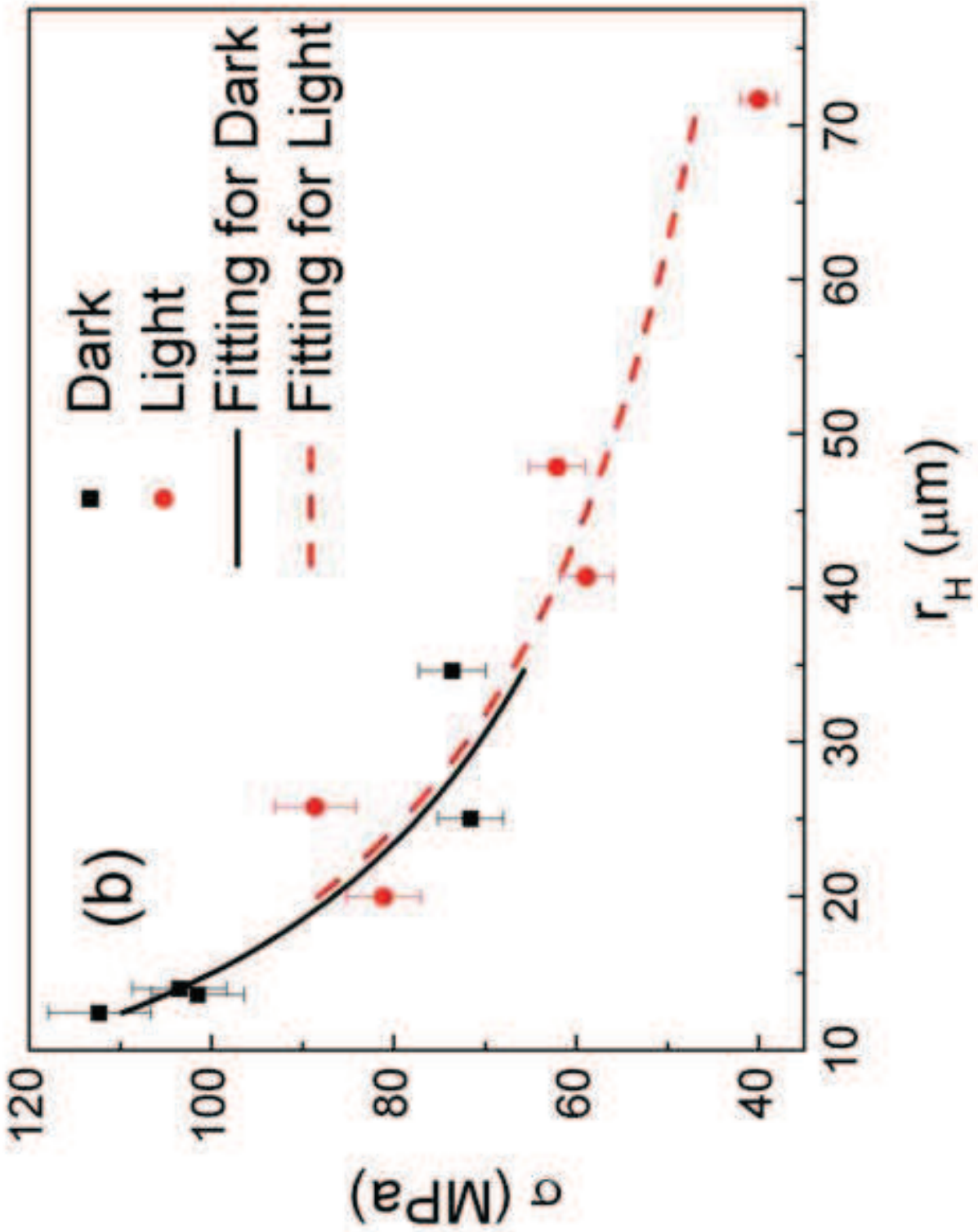
(b)
Dark
Light
Fitting for Dark
Fitting for Light
σ (MPa)
120
100
80
60
40
10
20
30
40
50
60
70
r_H (μm)

Figure